



Behavioral portfolio optimization via cumulative prospect theory with a symmetric alternating direction method of multipliers

Zhongming Wu¹ · Liu Yang¹ · Valentina De Simone²

Received: 15 March 2025 / Accepted: 22 July 2025

© The Author(s) 2025

Abstract

Amidst prevailing uncertainties in investment landscapes and heterogeneous investor risk attitudes toward gains and losses, this study investigates behavioral portfolio selection under a flexible investment horizon. We employ cumulative prospect theory (CPT) to model preferences, integrating mean-variance criteria with asymmetric risk behaviors. By extending the mean-variance framework, our model balances exploiting existing opportunities and exploring new assets to derive adaptive strategies. The optimization problem is solved using the symmetric alternating direction method of multipliers and the pooling-adjacent-violators algorithm, chosen for their efficacy in handling non-convexity and ordinal constraints. The optimal number of new assets to explore is determined via an integer programming problem, solved with a modified particle swarm optimization algorithm. In addition, we incorporate environmental, social, and governance (ESG) metrics to evaluate their impact on sustainable behavioral portfolios. Empirical analyses using real-world equity datasets demonstrate that strategic exploration enhances returns, reduces portfolio risk, and improves investment efficiency. The effectiveness of the proposed algorithm is also illustrated. The results highlight the value of adaptive horizon planning, ESG integration, and CPT preferences in portfolio optimization, offering actionable insights for investors navigating dynamic markets.

Keywords Portfolio optimization · Exploration of new assets · Cumulative prospect theory · ESG · Symmetric alternating direction method of multipliers

Extended author information available on the last page of the article

1 Introduction

In the sphere of investment management, both academics and professionals have dedicated considerable effort to understanding and effectively addressing the irrational behavior exhibited by investors [1]. Examining how varying attitudes towards gains and losses impact investment decision-making [2] is of particular interest. Although the traditional mean-variance portfolio model plays a central role in asset allocation, it does not adequately account for the psychological and emotional aspects of investors [3]. Furthermore, events such as the financial crisis and the outbreak of the COVID-19 pandemic have injected significant uncertainty into the investment landscape, resulting in profound changes in market dynamics [4]. Yields on fixed-income assets have markedly declined while corporate debt levels have surged. These factors have motivated investors to actively search for new investment instruments and prospects [5]. To mitigate this deficiency, this paper proposes a holistic approach that integrates the utility function of cumulative prospect theory into the conventional portfolio selection problem, resulting in the development of a behavioral portfolio selection model with an expandable investment horizon.

Cumulative prospect theory (CPT) [6, 7] stands as a highly regarded model within the realm of behavioral economics, offering valuable insights into decision-making processes in the presence of risk and uncertainty. This theory carries substantial implications for understanding and predicting investor behavior, market dynamics, and financial market anomalies. CPT exhibits four distinctive characteristics. First, individuals assess random outcomes as gains or losses relative to a specific reference point; Second, their aversion to losses greatly exceeds their inclination toward gains of equivalent magnitude, signifying loss aversion; Third, they display heightened sensitivity to the risks associated with low-probability events and are more inclined to accept the risks of high-probability events, thus manifesting a proclivity for risk losses; Fourth, they tend to assign higher subjective weight to low-probability events. Cumulative prospect theory is a pivotal component of behavioral finance research, occupying a prominent status within this domain. It finds applications in elucidating and forecasting investor behavior, market oscillations, and anomalies in financial markets. Its widespread utilization extends to diverse domains including equity allocation [8], efficiency assessment [9], and the formulation of consumer behavior models [10].

The evolution of investment methodologies rooted in CPT has impelled scholars to incorporate CPT into the context of portfolio selection seamlessly. For instance, Shefrin and Statman [11] introduced positive behavioral portfolio theory and explored its implications on portfolio construction and security design. Luxenberg et al. [12] devised optimal portfolio selection strategies based on CPT. Shi et al. [13] developed and analyzed three multi-period behavioral portfolio selection models grounded in cumulative prospect theory. Moreover, certain scholars have amalgamated behavioral finance theories with conventional models, culminating in more comprehensive and practical portfolio selection models, thereby offering a fresh perspective to financial theory and practice. Hens and Mayer [14] conducted a comparative analysis of asset allocations derived from CPT using two distinct approaches: one maximizing CPT based on a mean-variance efficient frontier, and another maximizing CPT with-

out this constraint. Fulga [15] proposed an integrated approach to portfolio selection, emphasizing the incorporation of investor preferences within an average risk framework to capture the genuine behavior of loss-averse investors better. Bi et al. [16] constructed a behavioral mean-variance model by introducing probability distortion into the traditional mean-variance portfolio selection problem, thereby accommodating investors' biases in probability judgment and aligning the model more closely with real-world scenarios.

For portfolio selection, the common assumption posits an investment universe comprising a risk-free asset and N risky assets [17, 18]. However, empirical applications reveal that even with a large N , the $N + 1$ assets predefined within the investment field do not encompass all potential opportunities, especially during zero- and negative-interest rate periods. Consequently, portfolio selection becomes intricate, demanding meticulous deliberation on the optimal balance between existing and newly discovered opportunities. Research on exploratory behavior underscores the challenge of making decisions in unpredictable environments, necessitating investors to strike a harmonious balance between exploring new prospects and representing all potential investment opportunities. This balance empowers investors to respond flexibly to market fluctuations, maximizing returns and enhancing performance [19, 20]. For instance, Aquino et al. [5] proposed a portfolio model wherein investors grapple with the trade-off between exploiting existing opportunities and representing all potential avenues. This approach aids investors in adapting to dynamic market conditions, identifying new prospects, and enhancing overall performance. Consequently, in portfolio optimization, it becomes imperative to integrate the exploration of new opportunities with the representation of all potential avenues. In this paper, we remove the constraint of a predetermined number of investment opportunities, contending that investors can expand their horizons by exploring new assets. If an exploration decision is made, investors allocate a portion of their wealth, representing exploration costs. The remaining wealth is then allocated to expanded assets, facilitating the construction of an optimal investment portfolio.

Recognizing the systematic inadequacy of traditional portfolio theory in explaining investor behavior during market turbulence, as well as the limitations of fixed assets allocation frameworks in adapting to rapidly evolving financial environments, this study integrates behavioral finance principles with asset exploration mechanisms to develop an optimized investment model that better reflects real-world decision-making processes. Specifically, we introduce a novel behavioral portfolio selection model that dynamically adapts to an expandable investment horizon, bridging the gap between traditional mean-variance portfolio optimization [21–24] and the empirically grounded insights of CPT. The contributions of our work are fourfold.

- We develop a behavioral portfolio optimization model by embedding the CPT utility function within the mean variance framework, which captures the asymmetric risk attitudes of investors, risk aversion in gains and risk seeking behavior in losses, while retaining the analytical tractability of conventional portfolio optimization. This dual incorporation enables a realistic representation of decision-making under uncertainty, addressing the limitations of symmetric risk in classical models.

- We propose a mechanism that optimizes resource allocation between exploiting existing assets and exploring untapped ones. The optimal number of new assets to explore is determined by integer programming. Then, the optimal portfolios incorporating this exploration are achieved via a non-convex mean-variance optimization problem. This strategy ensures flexibility in response to shifting market dynamics while preserving portfolio stability.
- We devise a computationally efficient solution framework to tackle the non-convex, non-smooth nature of the proposed optimization models. Specifically, a proximal SADMM is developed to handle rank-deficient return matrices and non-positive definite covariance structures arising from new asset integration, ensuring numerical stability. The pooling-adjacent-violators algorithm is leveraged to resolve the nonlinearity of the CPT utility, enabling the solvability of the subproblems.
- We conduct a rigorous convergence analysis for the proposed proximal SADMM, confirming its effectiveness in solving the behavioral portfolio selection problem within non-standard problem structures. The performance and efficiency of the new model and its solution method are further exemplified through a series of numerical experiments conducted on various real-world datasets.

The remainder of this paper is structured as follows. Section 2 offers a succinct overview of CPT. In Sect. 3, we develop an integer programming model to ascertain the optimal number of new assets to explore. Section 4 presents the formulation of a CPT-based behavioral portfolio optimization model, tailored for the exploitation of existing and new assets, along with the solution method. Section 5 extends our model to incorporate ESG factors. The empirical results of our experimental analysis are reported in Sect. 6. Concluding remarks are provided in Sect. 7.

1.1 Notation

Throughout the paper, we use \mathbb{N} , \mathbb{R} , \mathbb{R}^n , and $\mathbb{R}^{m \times n}$ to denote the sets of non-negative integers, real numbers, n -dimensional real column vectors, and $m \times n$ real matrices, respectively. For any $w, v \in \mathbb{R}^n$, the notation $\langle w, v \rangle = w^\top v$ signifies their inner product, and $\|w\| = \sqrt{\langle w, w \rangle}$ represents the Euclidean norm of w , where the superscript \top denotes transpose. When dealing with a symmetric matrix M , we define $\|w\|_M^2 = w^\top M w$. It is important to note that, following this convention, $\|w\|_M^2$ may not be nonnegative unless M is a positive definite matrix ($\succ 0$). Throughout the paper, we utilize I and 0 to denote the identity matrix and the zero vector with the appropriate dimensions. For a continuous function f , we use f' to denote its gradient.

2 Cumulative prospect theory

In the decision-making problem under cumulative prospect theory (CPT), the utility function and the probability weighting function are key components that characterize the preferences of the decision-maker [7].

Let Z be a random variable representing possible outcomes, with probability density function $f_Z(z)$ and cumulative distribution function $F_Z(z)$. The utility function U is a piecewise function that captures the subjective assessment of outcomes, defined by

$$U(z) = \begin{cases} -\mu(B - z)^\alpha, & z \leq B, \\ (z - B)^\varrho, & z > B, \end{cases}$$

where α and ϱ are the exponents for losses and gains, respectively, $\mu > 1$ is a parameter capturing the investor's loss aversion, and B is the reference point that defines gains and losses. The utility function is concave for gains and convex for losses, so that there is "decreasing sensitivity" in value as one moves away from the reference level B .

The probability weighting function $\omega : [0, 1] \rightarrow [0, 1]$, which models how individuals perceive probabilities nonlinearly leading to systematic deviations from rational decision-making under uncertainty, is defined by

$$\begin{aligned} \omega_-(F_Z(z)) &= \frac{F_Z(z)^\delta}{((1 - F_Z(z))^\delta + F_Z(z)^\delta)^{1/\delta}}, & z \leq B, \\ \omega_+(1 - F_Z(z)) &= \frac{(1 - F_Z(z))^\gamma}{((1 - F_Z(z))^\gamma + F_Z(z)^\gamma)^{1/\gamma}}, & z > B, \end{aligned} \quad (1)$$

where δ is the probability distortion parameter for losses, and γ is the probability distortion parameter for gains. In the loss domain, the weighting function $\omega_-(F_Z(z))$ distorts the cumulative distribution function $F_Z(z)$, where $\delta < 1$ indicates that decision makers assign higher subjective probabilities to smaller outcomes than their corresponding objective probabilities. In contrast, in the gain domain, $\omega_+(1 - F_Z(z))$ distorts the survival function $1 - F_Z(z)$, with $\gamma < 1$ implying overestimation of subjective probabilities relative to objective probabilities for larger outcome capture behavioral tendencies, including the overestimation of rare events and the underestimation of medium to high probabilities, leading to reduced sensitivity to differences in probabilities in the midrange.

Figure 1 visualizes the utility function and the probability weighting function of CPT. The S-shaped value function (left) shows greater sensitivity to losses ($\mu = 2.25$) than gains, with risk-seeking ($\alpha = 0.88$) and risk-averse ($\varrho = 0.88$) behaviors in respective domains. The probability weighting functions (right) demonstrate overweighting of small probabilities in losses ($\delta = 0.61$) and gains ($\gamma = 0.69$). These parametric specifications capture the essential behavioral patterns of loss aversion, diminishing sensitivity, and non-linear probability weighting that characterize CPT's explanatory framework.

Using the above notations for the general utility function and the probability weighting function, the decision problem within the CPT model can be reformulated as follows:

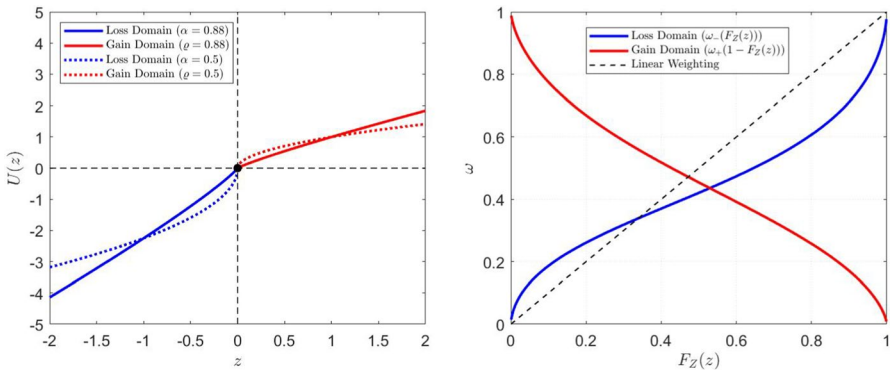


Fig. 1 An illustrate example for the utility function and probability weighting function of CPT

$$\max_{\mathbf{x}} \int_B^{+\infty} U(z) d[-\omega_+ (1 - F_Z(z))] + \int_{-\infty}^B U(z) d\omega_- (F_Z(z)) \quad \text{s.t. } z = \mathbf{r}^T \mathbf{x}, \quad \mathbf{x} \in \mathcal{X}, \quad (2)$$

where \mathbf{r} is a d -dimensional random return vector, and \mathcal{X} is the feasible set for decision variable \mathbf{x} . This optimization problem aims to maximize the expected utility of a random variable Z , which is represented as a linear function of the decision vector \mathbf{x} . The goal is to select a \mathbf{x} in a way that maximizes the expected value of the utility function $U(z)$, taking into account the probability that Z exceeds certain thresholds. The likelihood of Z exceeding a particular value z is captured by $1 - F_Z(z)$.

Let q_ν be the ν -th quantile of z , where $\nu \in (0, 1)$. Similar to the derivation in [25], we can approximate the distribution of z via either historical data or sample points generated by simulation. Specifically, given N realizations of \mathbf{r} , the estimated distribution of z is determined by the realizations of \mathbf{r} . Consequently, as discussed in [25], we can obtain the discretization problem of (2) as follows:

$$\min_{\mathbf{x}} - \sum_{i=1}^N \alpha_i U((R\mathbf{x})_{[i]}) \quad \text{s.t. } \mathbf{x} \in \mathcal{X}, \quad (3)$$

where $R \in \mathbb{R}^{N \times d}$ is the matrix formed by N scenarios of return vector \mathbf{r} , $(R\mathbf{x})_{[i]}$ is the i th smallest component of $R\mathbf{x}$, and α_i is the rank-dependent weight on $(R\mathbf{x})_{[i]}$, defined by $\alpha_i := \alpha_i(q_{\frac{i}{N}}) = [\omega_-(\frac{i}{N}) - \omega_-(\frac{i-1}{N})]1_{\{q_{\frac{i}{N}} \leq B\}} + [\omega_+(\frac{i-1}{N}) - \omega_+(\frac{i}{N})]1_{\{q_{\frac{i}{N}} > B\}}$,

where $1_{\{\cdot\}}$ is the characteristic function. This indicates that α_i takes on two distinct values on either side of B . The difficulty of this problem stems from the possible non-concavity and non-smoothness of U , the non-concavity induced by ω , and the rank of $(R\mathbf{x})_{[i]}$.

3 Optimal exploration number for new investment assets

Before integrating the CPT utility into portfolio optimization while exploring new assets, we must first determine the optimal number of explorations. This section aims to address this challenge by formulating an integer programming problem. Moreover, we employ a modified particle swarm optimization (PSO) algorithm to solve the resulting problem.

3.1 Mathematical formulation

Our investment framework considers m existing known risk assets (e.g., individual stocks or portfolios). Additionally, we can explore new assets on top of the existing ones, resulting in a total of d assets. The amount allocated for exploration is denoted by κ . The differentiating factor of the newly discovered asset compared to those in the existing investment universe is the associated cost of its discovery and the knowledge about its distributional properties. In contrast, the assets in the existing investment universe are readily available, and their distributional properties are well understood from the outset.

An investor allocates their wealth among these assets using a portfolio weight vector $\mathbf{x} = [x_1, \dots, x_m, x_{m+1}, \dots, x_{m+d}]^\top$, where $\mathbf{x}^h = [x_1, \dots, x_m]^\top$ represents the weight vector of the known risk assets, $\mathbf{x}^e = [x_{m+1}, \dots, x_{m+d}]^\top$ represents the weight vector of the new risk assets. The initial wealth is denoted as ξ_{init} . We impose a short selling constraint such that $x_i \geq 0$ for $i = 1, 2, \dots, m + d$. The return vector of the portfolio is given by $\mathbf{r} = [r_1, \dots, r_m, r_{m+1}, \dots, r_{m+d}]^\top$. Here, $\mathbf{r}^h = [r_1, \dots, r_m]^\top$ represents the return vector of the known risk assets, $\mathbf{r}^e = [r_{m+1}, \dots, r_{m+d}]^\top$ represents the return vector of the new risk assets. To represent the scenarios of return, we introduce the matrix $R \in \mathbb{R}^{N \times (m+d)}$, where N is the number of scenarios. Each row of R , denoted by \mathbf{r}_i^\top , represents the return vector for scenario i , $i = 1, 2, \dots, N$. The mean return vector for scenario i is given by $\boldsymbol{\mu}_i = \mathbb{E}[\mathbf{r}_i]$, and the covariance matrix of the total risk asset's returns for scenario i , with dimensions $(m + d) \times (m + d)$, is denoted as $\mathbf{C}_i = \mathbb{E}[(\mathbf{r}_i - \boldsymbol{\mu}_i)(\mathbf{r}_i - \boldsymbol{\mu}_i)^\top]$.

In our analysis, we allow the exploration of any number of new assets, denoted by $d \in \mathbb{N}_0$. The agent's objective is to concurrently determine whether to exercise the option to explore new investment opportunities and, if the option is exercised, to specify the number of new assets to explore and an optimal allocation in the extended investment universe. To determine the optimal number d of new assets and optimal investment strategy, we promote a CPT-based behavioral portfolio optimization problem with an uncertain number of new assets to explore. The number d of new assets to explore is a decision variable. In this setting, exploring a new asset comes at a fixed cost $\kappa > 0$. We define $\bar{r}_l^e, l = 1, \dots, d$, as the expected returns and $s_l^e, l = 1, \dots, d$, as the standard deviation of the newly discovered assets. The statistical properties of the newly discovered assets are chosen according to the recursion [5]:

$$\bar{r}_1^e = 1.25, \quad s_1^e = 0.3,$$

$$\bar{r}_l^e = \max \left\{ 1, \bar{r}_{l-1}^e - \frac{0.1}{l^2} \right\}, \text{ and } s_l^e = s_{l-1}^e - \frac{0.1}{l^2}, \quad l = 2, 3, \dots, d. \quad (4)$$

Note that the recursive expressions in (4) yield a sequence of assets with decreasing Sharpe ratios, i.e., $\frac{\bar{r}_j^e - r_f}{s_j^e} > \frac{\bar{r}_{j+1}^e - r_f}{s_{j+1}^e}$, for $j \in \mathbb{N}$, where $r_f \in \mathbb{R}$ is risk-free rate. This property reflects the intuition that the agent discovers “low-hanging fruits” first and that it becomes increasingly difficult to find new profitable opportunities.

Building on the methodology introduced by Aquino et al. [5], we use $\tilde{D}_e(d)$ to characterize the optimal risk-adjusted return achievable within the mean-variance framework under specific market conditions. The performance of the extended portfolio is evaluated by analyzing the metric $\tilde{D}_e(d)$, with the results summarized as follows:

$$\begin{aligned} \tilde{D}_e(d) = & \sum_{i=1}^N \left(\sum_{i=1}^m \sum_{j=1}^m \bar{C}_{i,j}^{-1} (r_i^h - r_f) (r_j^h - r_f) + 2 \sum_{i=1}^m \sum_{j=1}^d \bar{C}_{i,m+j}^{-1} (r_i^h - r_f) (\bar{r}_j^e - r_f) \right. \\ & \left. + \sum_{i=1}^d \sum_{j=1}^d \bar{C}_{m+i,m+j}^{-1} (\bar{r}_i^e - r_f) (\bar{r}_j^e - r_f) \right), \end{aligned} \quad (5)$$

where \bar{C} represents the covariance matrix of known and newly acquired assets and $r_f \in \mathbb{R}$ is risk-free rate. Considering the initial wealth and the exploration cost of new assets, the discrete decision variable d that optimally minimizes (5) is determined by

$$\min_d -\tilde{D}_e(d) \quad \text{s.t. } \kappa d \leq \xi_{init}, \quad d \in \mathbb{N}, \quad (6)$$

where κ is a fixed exploration cost. Since $\tilde{D}_e(d)$ is neither a linear nor a monotone function with respect to the exploration number d , model (6) turns into a nonlinear integer programming problem that requires specific solution methods.

3.2 PSO for solving model (6)

In this subsection, we propose a modified PSO algorithm to solve model (6) and obtain the optimal value of d^* . It is essential to recognize that, due to the investment portfolio’s budget constraints, the optimal number of new assets needs to be determined while minimizing exploration costs. Given these constraints, minimizing exploration costs is crucial when identifying d^* . However, because the decision variable is discrete and the objective function is complex, we adopt the PSO algorithm as a reliable optimization method to solve this problem efficiently.

The PSO algorithm is a nature-inspired meta-heuristic optimization algorithm. It was developed by drawing inspiration from the social behavior of bird flocking or fish schooling. In PSO, a swarm of particles is initialized in the search space. Each particle represents a potential solution to the optimization problem. For example,

in a function optimization problem, a particle's position in the search space corresponds to a set of input values for the function. Each particle has a position vector and a velocity vector. The position of a particle is updated based on its velocity, and the velocity is adjusted according to the particle's own experience (personal best position) and the experience of the entire swarm (global best position). The implementation is governed by several parameters, including the swarm size n , maximum iteration counts K_{\max} , inertia weight ϖ , cognitive coefficient ς_1 , social coefficient ς_2 , and maximum velocity ϑ_{\max} , which collectively dictate the algorithm's convergence properties and balance between exploration and exploitation. Algorithm 1 provides the pseudocode of PSO for solving model (6).

- 1: **Input:** Objective function $-\tilde{D}_e(d)$, number of particles n , maximum iterations K , inertia weight $\varpi > 0$, acceleration coefficients $\varsigma_1, \varsigma_2 > 0$, generate random vectors $o_1, o_2 \sim U(0, 1)$ for all particles, position bounds (d_{\min}, d_{\max}) , velocity bounds $(\vartheta_{\min}, \vartheta_{\max})$.
- 2: Initialize particle positions d_i^0 and velocities ϑ_i^0 randomly within the given bounds.
- 3: Evaluate the fitness $-\tilde{D}_e(d_i^0)$ for each particle.
- 4: Set the personal best positions $p_i^0 = d_i^0$ and update global best g^0 .
- 5: **for** $k = 1$ to K , **do**
- 6: **for** each particle i , **do**
- 7: Update velocity:

$$\vartheta_i^k = \varpi \vartheta_i^{k-1} + \varsigma_1 o_1 (p_i^{k-1} - d_i^{k-1}) + \varsigma_2 o_2 (g^{k-1} - d_i^{k-1}).$$
- 8: Apply velocity bounds: $\vartheta_i^k = \max\{\vartheta_{\min}, \min\{\vartheta_i^k, \vartheta_{\max}\}\}$.
- 9: Update position: $d_i^k = d_i^{k-1} + \vartheta_i^k$.
- 10: Apply position bounds: $d_i^k = \max\{d_{\min}, \min\{d_i^k, d_{\max}\}\}$.
- 11: Evaluate fitness $-\tilde{D}_e(d_i^k)$.
- 12: Update personal best:

$$\text{if } -\tilde{D}_e(d_i^k) < -\tilde{D}_e(p_i^{k-1}), \text{ then } p_i^k = d_i^k.$$

Otherwise, $p_i^k = p_i^{k-1}$.
- 13: **end for**
- 14: Update global best:

$$g^k = \arg \min_{p_i^k} -\tilde{D}_e(p_i^k).$$
- 15: **end for**
- 16: Return global best position $d^* = g^k$ and fitness $-\tilde{D}_e(d^*)$.
- 17: **Output:** Best solution d^* and its fitness value $-\tilde{D}_e(d^*)$.

Algorithm 1 PSO for solving model (6)

3.3 An illustrate example

To validate the effectiveness of the PSO algorithm, we present a numerical example in which the expected return matrix of the existing risky assets is given as follows:

$$r^h = \begin{bmatrix} 1.162 & 1.246 & 0.8357 \\ 1.312 & 0.9073 & 1.1913 \\ 0.9519 & 1.2761 & 0.996 \end{bmatrix}.$$

Given that the initial wealth is $\xi_{init} = 1$, and we assume that the exploration cost for each new asset is $\kappa = 0.03$. Then, the value of d is constrained to the range $[1, 33]$, with 33 being the rounded value of $1/0.03$. We use the PSO algorithm (Algorithm 1) to solve this example. The parameters utilized for the PSO implementation include a swarm size of $n = 10$, a maximum number of iterations $K_{\max} = 100$, an inertia weight $\varpi = 0.5$, a cognitive coefficient $\varsigma_1 = 1.5$, a social coefficient $\varsigma_2 = 1.5$, a minimum velocity $\vartheta_{\min} = -5$, a maximum velocity $\vartheta_{\max} = 5$, and initial value $\vartheta_i^0 = 0$. Fig. 2 illustrates the variation of $-\tilde{D}_e(d)$ across discrete values of d , clearly showing a trend in the performance metric.

In Fig. 2, the red marker highlights the optimal solution d^* , determined through the PSO algorithm. The plot demonstrates the algorithm's effectiveness in identifying the point where $-\tilde{D}_e(d)$ is minimized, reflecting the optimal risk-adjusted return under the given constraints. The optimization results demonstrated that the algorithm efficiently converged to the optimal value d^* within fewer than 50 iterations, with an exploration range bounded by $d_{\min} = 0$ and $d_{\max} = 33$. The discrete and bounded nature of d constrained the search space, enabling the PSO algorithm to effectively minimize the performance metric $-\tilde{D}_e(d)$ while adhering to the imposed constraints.

The objective function $-\tilde{D}_e(d)$ evolves dynamically with d , as it recursively updates the expected returns \bar{r}_l^e and standard deviations s_l^e for new assets. These updates, in turn, modify the covariance matrix \bar{C} , which influences the risk-return tradeoff. The PSO algorithm demonstrated its adaptability to this evolving optimiza-

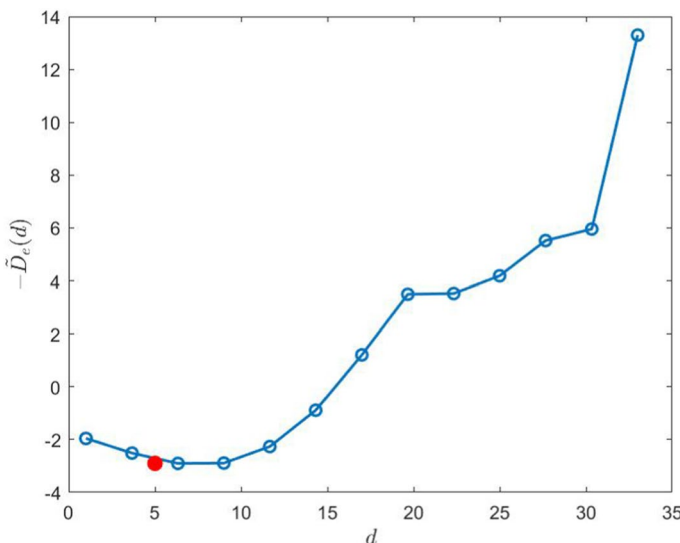


Fig. 2 Plot of $-\tilde{D}_e(d)$ values with the optimal solution d^* highlighted in red

tion landscape by effectively utilizing both its global exploration and local exploitation capabilities to identify the optimal solution.

4 CPT-based behavioral portfolio optimization with exploration of new assets

In this section, we introduce a behavioral portfolio optimization framework that integrates the exploration of new investment assets. Specifically, the new model allows investors to allocate resources to new assets while considering exploration costs and budget constraints. It is designed to balance the trade-off between exploiting known assets and exploring new opportunities, incorporating investor behavioral preferences under the CPT. Subsequently, we employ the symmetric alternating direction method of multipliers (SADMM) to address the proposed model. Besides, due to the non-convex and non-smooth nature of the CPT utility function, we leverage the pooling-adjacent-violator (PAV) algorithm to solve one of the subproblems efficiently. The convergence of the developed algorithm is also rigorously analyzed.

4.1 CPT-based behavioral portfolio model with exploration

After determining the optimal number of new assets to explore, we propose a mechanism for optimizing resource allocation between existing and new assets. As discussed in Sect. 2, the CPT utility can capture investors' asymmetric risk attitudes, namely risk-aversion when facing gains and risk-seeking behavior when dealing with losses. Rather than relying on the traditional mean-variance framework, we utilize the CPT utility function to represent investors' returns and develop a novel behavioral portfolio optimization framework that incorporates the exploration of new assets.

Concretely, we propose a CPT-based behavioral portfolio model with exploration of new investment assets as follows:

$$\min_{\mathbf{x}} \quad \sum_{i=1}^N \mathbf{x}^\top C_i \mathbf{x} - \sum_{i=1}^N \alpha_i U((R\mathbf{x})_{[i]}) \quad \text{s.t. } \mathbf{x} \in \mathcal{X}, \quad (7)$$

where \mathcal{X} is the feasible set for decision variable \mathbf{x} , defined by $\mathcal{X} = \{\mathbf{x} : x_i \geq 0, i = 1, 2, \dots, m + d^*, \sum_{i=1}^{m+d^*} x_i + \kappa d^* = \xi_{init}\}$. The first constraint in \mathcal{X} is the short-selling constraint of the risky asset, while the second constraint is the budget constraint, where the amount devoted to exploration κd^* , expressed as a monetary amount, is a part of the initial wealth ξ_{init} at the stage of the portfolio optimization problem. The parameter α_i can also be seen as a balance between utility and variance-based risk.

Since the objective function is non-convex and non-smooth, model (7) cannot be solved using common solvers and classical constrained optimization methods. Subsequently, inspired by the approach developed in [25–27], we propose a SADMM to solve model (7).

4.2 SADMM for solving model (7)

It is well known that alternating direction method of multipliers (ADMM) is an efficient first-order optimization method, and its theory and application have been extensively reviewed in the literature [28–30]. ADMM was firstly proposed by Gabay and Mercier [31] and has gained popularity in solving various practical problems. The fundamental concept of ADMM involves the alternate updating of the original pairwise variables within the augmented Lagrangian function associated with the optimization problem. To enhance the convergence speed of ADMM, He et al. [32, 33] introduced the symmetric alternating direction method of multipliers (SADMM), which updates the Lagrangian multiplier more than once in each iteration. This algorithm subsumes ADMM as a special case. For tackling the problem of minimizing the sum of two non-convex functions with linear constraints, Wu et al. [27] proposed a variation of the SADMM, incorporating the classic ADMM into the algorithmic framework. To address the non-convex and non-smooth nature of maximizing portfolio utility, Jing et al. [34] developed a hybrid derivative-free optimization algorithm that incorporates ADMM. Given the non-convex and non-smooth nature of the CPT utility function, this paper adopts a variant of the SADMM [27] to solve model (7).

The SADMM is typically employed to solve optimization problems with the following structure [35]:

$$\begin{aligned} & \min_{w,v} f(w) + g(v) \\ & \text{s.t. } Ew + Fv = b, \end{aligned} \tag{8}$$

where f and g are non-convex functions and E, F and b are known matrices and vectors. The specific iteration scheme of SADMM to solve (8) can be read as

$$\left\{ \begin{array}{l} w^{k+1} = \operatorname{argmin}_w L_\sigma(w, v^k; \lambda^k), \\ \lambda^{k+\frac{1}{2}} = \lambda^k - \theta\sigma(Ew^{k+1} + Fv^k - b), \\ v^{k+1} = \operatorname{argmin}_v L_\sigma(w^{k+1}, v; \lambda^{k+\frac{1}{2}}), \\ \lambda^{k+1} = \lambda^{k+\frac{1}{2}} - \sigma(Ew^{k+1} + Fv^{k+1} - b), \end{array} \right.$$

where $\theta \in (-1, 1)$ is a relaxation factor, σ is a penalty parameter, and L_σ denotes the augmented Lagrangian function associated with problem (8) defined by

$$L_\sigma(w, v; \lambda) = f(w) + g(v) - \langle \lambda, Ew + Fv - b \rangle + \frac{\sigma}{2} \|Ew + Fv - b\|_2^2.$$

Note that SADMM is a generalization of ADMM, a method extensively studied in convex and nonconvex optimization [25, 26, 30, 36, 37]. Specifically, SADMM is reduced to ADMM when $\theta = 0$.

Next, we apply the aforementioned SADMM to solve the CPT-based model involving the of new investment assets, as presented in the previous section. The primary challenge in optimizing (7), as emphasized by Cui et al. [25], stems from

the non-smoothness and non-convexity of the utility function. The non-smoothness arises from the order statistics of Rx , representing a finite realization of the terminal wealth. Meanwhile, the non-convexity is attributed to the S-shaped utility. Additionally, a more subtle challenge arises from the probability distortion (1) and the ranked realization of the terminal wealth, which introduces further non-convexity and non-smoothness, depending on the final wealth value and the reference point B . To address the difficulty posed by the utility function, we introduce an auxiliary variable $y \in \mathbb{R}^N$ to represent terminal wealth realizations. As a result, we reformulate problem (7) as follows:

$$\min_{\mathbf{x}, \mathbf{y}} \sum_{i=1}^N \mathbf{x}^\top C_i \mathbf{x} - \sum_{i=1}^N \alpha_i U(y_{[i]}) + I_{\mathcal{X}}(\mathbf{x}) \quad \text{s.t. } \mathbf{y} = Rx, \quad (9)$$

where $I_{\mathcal{X}}$ is the indicator function of the set \mathcal{X} , that is, $I_{\mathcal{X}}(\mathbf{x}) = 0$ if $\mathbf{x} \in \mathcal{X}$ and ∞ otherwise. The augmented Lagrangian function of problem (9) is

$$L_\sigma(\mathbf{x}, \mathbf{y}; \boldsymbol{\lambda}) = \sum_{i=1}^N \mathbf{x}^\top C_i \mathbf{x} - \sum_{i=1}^N \alpha_i U(y_{[i]}) + I_{\mathcal{X}}(\mathbf{x}) + \langle \boldsymbol{\lambda}, \mathbf{y} - Rx \rangle + \frac{\sigma}{2} \|\mathbf{y} - Rx\|_2^2. \quad (10)$$

In the given framework, the augmented Lagrangian function involves two variables, namely \mathbf{x} and \mathbf{y} , with $\boldsymbol{\lambda}$ serving as the Lagrangian multiplier, and $\sigma > 0$ representing the quadratic penalty parameter [38]. The SADMM is utilized as a strategy to update the original and paired iteratively variables within the augmented Lagrangian function associated with the optimization problem [39].

By leveraging SADMM, we can efficiently optimize both variables simultaneously. The update steps of SADMM are outlined below:

$$\mathbf{x}^{k+1} = \operatorname{argmin}_{\mathbf{x} \in \mathcal{X}} L_\sigma(\mathbf{x}, \mathbf{y}^k; \boldsymbol{\lambda}^k) + \frac{1}{2} \|\mathbf{x} - \mathbf{x}^k\|_M^2, \quad (11a)$$

$$\boldsymbol{\lambda}^{k+\frac{1}{2}} = \boldsymbol{\lambda}^k + \theta \sigma (\mathbf{y}^k - Rx^{k+1}) \quad (11b)$$

$$\mathbf{y}^{k+1} = \operatorname{argmin}_{\mathbf{y}} L_\sigma(\mathbf{x}^{k+1}, \mathbf{y}; \boldsymbol{\lambda}^{k+\frac{1}{2}}), \quad (11c)$$

$$\boldsymbol{\lambda}^{k+1} = \boldsymbol{\lambda}^{k+\frac{1}{2}} + \sigma (\mathbf{y}^{k+1} - Rx^{k+1}). \quad (11d)$$

We summarize our SADMM framework for solving model (7) in Algorithm 2.

1: **Input:** Given R , σ , ϵ_1 , ϵ_2 , \mathbf{y}^0 , $\boldsymbol{\lambda}^0$, and $k = 0$. Choose $M = \eta\mathbf{I} - \sum_{i=1}^N 2C_i - \sigma R^\top R$ with $\eta > \lambda_{\max}(\sum_{i=1}^N 2C_i + \sigma R^\top R)$, where λ_{\max} denotes the maximum eigenvalue.
2: **for** $k = 0, 1, \dots$, **do**
3: Solve (11a) to obtain \mathbf{x}^{k+1} ;
4: Update $\boldsymbol{\lambda}^{k+\frac{1}{2}} = \boldsymbol{\lambda}^k + \theta\sigma(\mathbf{y}^k - R\mathbf{x}^{k+1})$;
5: Solve (11c) to obtain \mathbf{y}^{k+1} either exactly or approximately;
6: Update $\boldsymbol{\lambda}^{k+1} = \boldsymbol{\lambda}^{k+\frac{1}{2}} + \sigma(\mathbf{y}^{k+1} - R\mathbf{x}^{k+1})$.
7: If the stopping criteria $\frac{\|\mathbf{y}^k - R\mathbf{x}^k\|}{\|\mathbf{y}^k\|} \leq \epsilon_1$ and $\frac{\|\mathbf{y}^k - \mathbf{y}^{k+1}\|}{\|\mathbf{y}^k\|} \leq \epsilon_2$ are satisfied, return \mathbf{x}^k .
8: **end for**

Algorithm 2 SADMM for solving model (7)

Due to the introduction of new assets or when $m + d > N$ (indicating that the assets count realizations exceed the realizations), the covariance matrix C may lose positive definiteness. Consequently, ensuring the convexity of the x -subproblem becomes uncertain, imparting complexity to the algorithm. In efforts to refine the accuracy of the resolution of x -subproblems and accelerate convergence, we propose enhancements to the SADMM algorithm. Specifically, we integrate a proximal term into the x minimization subproblem of SADMM, approximating its solution and ensuring convexity overall for the x -subproblem [40]. In instances where \mathcal{X} denotes a polyhedron, the x -subproblem (11a) can be reformulated as a quadratic programming problem:

$$\min_{\mathbf{x} \in \mathcal{X}} \sum_{i=1}^N \mathbf{x}^\top C_i \mathbf{x} + \frac{\sigma}{2} \left\| \mathbf{y}^k - R\mathbf{x} + \frac{\boldsymbol{\lambda}^k}{\sigma} \right\|_2^2 + \frac{1}{2} \left\| \mathbf{x} - \mathbf{x}^k \right\|_M^2. \quad (12)$$

We choose the proximal matrix M to be $M = \eta\mathbf{I} - \sum_{i=1}^N 2C_i - \sigma R^\top R$, and the coefficient $\eta > 0$ in this context exceeds the maximum eigenvalue of the matrix $\sum_{i=1}^N 2C_i + \sigma R^\top R$. In this setting, we know that $M \succ 0$ and the x -subproblem (12) has the closed-form solution. This modification aims to leverage the structure of the polyhedral set \mathcal{X} and enhance the overall efficiency of the SADMM algorithm, especially in scenarios where the problem involves polyhedral constraints. The introduction of the proximal term contributes to achieving a more precise approximation of the solution, leading to accelerated convergence in the optimization process.

The primary challenge arises from the optimization of the y -subproblem (11c), which presents a non-convex and non-smooth optimization problem. To address this issue, Cui et al. [25] has proposed two effective algorithms that take advantage of the inherent structure of the y -subproblem. Further details are provided in Sect. 4.3. At the k -th iteration, the y -subproblem aims to minimize the following function:

$$\Phi(\mathbf{y}) = - \sum_{i=1}^N \alpha_i U(y_{[i]}) + \frac{\sigma}{2} \left\| \mathbf{y} - R\mathbf{x}^{k+1} + \frac{\boldsymbol{\lambda}^{k+\frac{1}{2}}}{\sigma} \right\|^2.$$

4.3 Solving y-subproblem in SADMM

In this section, we introduce the pooling-adjacent-violators (PAV) algorithm for addressing the y-subproblem. The PAV algorithm has demonstrated remarkable effectiveness in tackling separable convex optimization problems involving chain constraints. It was originally introduced by Ayer et al. [41] and subsequently extended by Brunk et al. [42] for maximum likelihood estimation (MLE) under chain constraints. Over the years, the PAV algorithm has found adaptation and application in various scenarios, as evidenced by its utilization by researchers such as Ahuja and Orlin [43] and Cui et al. [44]. Building upon this established foundation, Cui et al. [25] creatively proposed an algorithm rooted in the PAV framework to solve the CPT utility optimization problem with chain constraints. Despite the non-convex nature of (11c) and its reformulation, the efficient resolution of the y-subproblem is made possible by harnessing the unique structure of $f_i(y)$.

We introduce the reformulation of the y-subproblem by defining $w^{k+1} = Rx^{k+1} - \frac{\lambda^{k+\frac{1}{2}}}{\sigma}$. For simplicity, we omit the superscript in w^{k+1} in the remainder of this subsection. Let $\{l_1, l_2, \dots, l_N\}$ be a permutation of $\{1, 2, \dots, N\}$ such that $w_{l_1} \leq w_{l_2} \leq \dots \leq w_{l_N}$. Since $\alpha_i U(y_{[i]})$ remains independent of any permutation of y , after this transformation, the y-subproblem (11c) is equivalent to the following problem:

$$\min \sum_{i=1}^N f_i(y_{l_i}) \quad \text{s.t. } y_{l_1} \leq y_{l_2} \leq \dots \leq y_{l_N}, \quad (13)$$

where $f_i(y_{l_i}) = -\alpha_i U(y_{l_i}) + \frac{\sigma}{2}(y_{l_i} - w_{l_i})^2$. Without loss of generality, in this subsection, we assume $w_1 \leq w_2 \leq \dots \leq w_N$ for further simplicity of notations. Thus, problem (13) is equivalent to the following isotonic program:

$$\min \sum_{i=1}^N f_i(y_i) \quad \text{s.t. } y_1 \leq y_2 \leq \dots \leq y_N, \quad (14)$$

where $f_i(y_i) = -\alpha_i U(y_i) + \frac{\sigma}{2}(y_i - w_i)^2$, and the constraint in (14) adheres to the simple chain constraint as defined in the work of Best and Hlouskova [17].

Next, we briefly introduce the variants of the PAV algorithm by Cui et al. [25] for solving the y-subproblem. First, let the set $J = \{1, \dots, N\}$, and divide the set J into n blocks $[1, 1], [2, 2], \dots, [N, N]$, where each block $[p, q]$ is a continuous set of integers $\{p, p+1, \dots, q\}$. If every y_i in the optimal solution to the following problem has the same value, then the block $[p, q]$ is a single-valued block:

$$\min \sum_{i=p}^q f_i(y_i) \quad \text{s.t. } y_p \leq y_{p+1} \leq \dots \leq y_q,$$

i.e., $y_p^* = y_{p+1}^* = \dots = y_q^*$ and we define this value by $V_{[p,q]}$. If there are some adjacent blocks $[p, q]$ and $[q + 1, r]$ in J such that the monotonic constraint is violated, i.e., $V_{[p,q]} > V_{[q+1,r]}$, then we replace the blocks $[p, q]$ and $[q + 1, r]$ with the larger block $[p, r]$, thereby merging the two blocks. When there is no violation value in adjacent blocks, the optimal solution is given by $y_i = V_{[p,q]}$ for all $p \leq i \leq q$ and $[p, q] \in J$. The PAV algorithm terminates when all adjacent blocks have non-decreasing values. The pseudo-codes of the PAV algorithm for solving y-subproblem are summarized in Algorithm 3.

```

1: Input:  $J = \{[1, 1], [2, 2], \dots, [N, N]\}$ .
2: for  $i = 1, 2, \dots, N$ , do
3:   Compute the minimizer  $V_{[i,i]}$  of  $f_i(y_i)$ .
4: end for
5: while  $\exists [m, n], [n + 1, p] \in J$  such that  $V_{[m,n]} > V_{[n+1,p]}$ , do
6:    $J \leftarrow J \setminus \{[m, n], [n + 1, p]\} \cup \{[m, p]\}$ ;
7:   Compute the minimizer  $V_{[m,p]}$  of  $\sum_{i=m}^p f_i(y_i)$ .
8: end while
9: for each  $[m, n] \in J$ , do
10:  Update  $y_i = V_{[m,n]}, \forall i = m, m + 1, \dots, n$ .
11: end for
```

Algorithm 3 PAV algorithm for solving y-subproblem (11c)

It should be noted that the traditional PAV algorithm requires f_i to be a univariate convex function, but Cui et al. [25] proved that although f_i is non-convex, one can analyze the monotonicity of f_i to find its minimizer via binary search. In fact, $\sum_{i=p}^q f_i(y)$ has at most two local minimizers, and we can simply choose the minimizer with the smaller function value [25, Fact 1].

Lemma 1 Let y^* be an optimal solution of problem (14). Then, we have $U'(y_i^*) < \infty, \forall i = 1, 2, \dots, N$.

Lemma 1 establishes that the optimal solution to the y-subproblem must adhere to a condition ensuring the well-defined nature of the Clarke generalized gradient, as delineated in Lemma 3. This condition assumes a pivotal role in algorithmic design and associated convergence analysis.

Lemma 2 Let y^* be an optimal solution of problem (14). Then, we have

$$w_1 \leq y_1^* \leq \dots \leq y_N^* \leq \max_{i=1,\dots,N} \left\{ \max \left\{ B + 1, w_i + \frac{b_i U'(B + 1)}{\sigma} \right\} \right\}.$$

Furthermore, Lemma 2 delineates that the optimal solution to problem (14) is constrained by established constants, where

$$l_b = w_1 \quad \text{and} \quad u_b = \max_{i=1,\dots,N} \left\{ \max \left\{ B + 1, w_i + \frac{b_i U'(B + 1)}{\sigma} \right\} \right\}$$

serve as the initial lower and upper bounds for the PAV algorithm's solution to the y -subproblem. In our implementation, referring to Cui et al. [25], we employ binary search which maintains a search interval containing the optimal solution. In each iteration, the binary search performs a function evaluation to halve the search interval, iterating until a local minimum is found. This property proves instrumental in the convergence analysis of our algorithm.

Theorem 1 *The solution \bar{y} returned by the PAV algorithm satisfies $0 \in \partial\Gamma(\bar{y})$.*

Although the proposed variant of the PAV algorithm cannot be expected to converge to the global optimal solution, we prove in Theorem 1 that it generates a stationary point for the optimization problem defined as:

$$\min_y \Gamma(y) := \sum_{i=1}^N -\alpha_i U(y_{[i]}) + \frac{\sigma}{2} (y_{[i]} - w_i)^2, \quad (15)$$

where (15) corresponds to (14). For detailed proofs of the aforementioned Lemmas and Theorem, kindly refer to Cui et al. [25].

4.4 Convergence analysis of SADMM

In this subsection, we conduct a convergence analysis for SADMM. Let $\Omega(y) = -\sum_{i=1}^N \alpha_i U(y_{[i]})$, which constitutes the initial component of the function $\Phi(y)$. Notably, both $\Omega(y)$ and $\Phi(y)$ are locally Lipschitz functions, subject to specific mild conditions as outlined in Lemma 1 by Cui et al. [25]. Consequently, determining stationary points can be facilitated through the utilization of the Clarke generalized gradient. If $U'(y_i) < \infty, \forall i$, then the Clarke generalized gradient of $\Omega(y)$, denoted as $\partial\Omega(y)$, exists [45].

Lemma 3 (Outer semicontinuity) Let y be such that Ω is locally Lipschitz near y . Then, for any sequences $\{v^k\}$ and $\{y^k\}$ such that $v^k \rightarrow v^*, y^k \rightarrow y^*$ and $v^k \in \partial\Omega(y^k)$, we have $v^* \in \partial\Omega(y^*)$.

Assumption 1 Suppose x^* represents a local minimizer of (11a). In such a case, it can be inferred that 0 lies within the set defined by the relation:

$$0 \in R^\top \partial\Omega(Rx^*) + 2 \sum_{i=1}^N C_i x^* + M(x^* - x^k) + N_{\mathcal{X}}(x^*). \quad (16)$$

Note that $N_{\mathcal{X}}(\bar{x})$ denotes the normal cone of the set \mathcal{X} at the point $\bar{x} \in \mathcal{X}$. Mathematically, this normal cone is defined as: $N_{\mathcal{X}}(\bar{x}) = \{\nu \in \mathbb{R}^{m+d} \mid \langle \nu, x - \bar{x} \rangle \leq 0, \forall x \in \mathcal{X}\}$. Furthermore, it is pertinent to note that $\partial I_{\mathcal{X}}(x)$ is equivalent to $N_{\mathcal{X}}(x)$, as established

in Beck [46]. The proposed SADMM algorithm converges to a point satisfying the necessary optimality condition (16) under mild conditions.

Assumption 2 The x -subproblem is globally solved. The y -subproblem is resolved with the following conditions:

$$\begin{aligned} L_\sigma \left(x^{k+1}, y^k; \lambda^{k+\frac{1}{2}} \right) - L_\sigma \left(x^{k+1}, y^{k+1}; \lambda^{k+\frac{1}{2}} \right) &\geq 0, \quad \text{and} \\ 0 &\in \partial \Omega(y^{k+1}) + \sigma \left(y^{k+1} - Rx^{k+1} + \frac{\lambda^{k+\frac{1}{2}}}{\sigma} \right). \end{aligned} \quad (17)$$

Assumption 2 pertains to the solutions of the x - and y -subproblems. We remark that the above assumption is quite mild. When \mathcal{X} is a convex set and the proximal term is introduced, the x -subproblem becomes a convex programming problem, and obtaining its global solution is straightforward. Meanwhile, the y -subproblem possesses unique characteristics, it can only be solved to a stationary point, denoted as y^{k+1} , whose objective value does not surpass the point y^k . To address this, we employ the PAV algorithm for solving the y -subproblem that can return a solution satisfying (17), with a detailed introduction provided in Sect. 4.3.

Assumption 3 The sequence of Lagrangian multiplier $\{\lambda^k\}$ is bounded and satisfies $\sum_{k=0}^{\infty} \|\lambda^{k+1} - \lambda^k\|^2 < \infty$.

It is important to emphasize that detailed explanations of Lemma 3, Assumptions 1 and 2 are the same to those in Cui et al. [25]. Therefore, to maintain conciseness, we refrain from reiterating these prerequisites within the scope of this article. As remarked in [25], the convergence of non-convex ADMM with two non-smooth blocks is challenging without imposing assumptions such as Assumption 3; see, for example, [37, 47]. Additionally, it is worth noting that Assumption 3 is extensively utilized in the ADMM literature, as seen in works such as [40] and [48].

Subsequently, we will delve into the convergence properties and provide a proof for the SADMM.

Assumption 4 The sequence of $\{y^k\}$ is bounded and satisfies $\frac{\theta\sigma}{\theta+1} \sum_{k=0}^{\infty} \|y^{k+1} - y^k\|^2 < \infty$.

It is noteworthy that when θ is 0, Assumption 4 is not required; when θ is not 0, in order to ensure the convergence of the algorithm, we make the assumption.

Theorem 2 Assuming \mathcal{X} is a convex and closed set, $\epsilon_1 = \epsilon_2 = 0$, while Assumptions 2 and 3 are satisfied. Let $\{(x^k, y^k)\}$ be a sequence generated by the SADMM algo-

rithm. Then, any accumulation point of the sequence, denoted as (x^*, y^*) , satisfies the following condition:

$$0 \in R^\top \partial \Omega(y^*) + 2 \sum_{i=1}^N C_i x^* + M(x^* - x^k) + N_{\mathcal{X}}(x^*), \quad y^* = Rx^*.$$

Hence, x^* is a stationary point of (7) in the sense that Assumptions 1 hold.

Proof The first-order optimality condition of the x -subproblem (11a) in Algorithm 2 can be read as

$$\eta x = R^\top \lambda^k + \sigma R^\top y^k + Mx^k.$$

Since the x -subproblem is strongly convex with $\eta > 0$, we have

$$L_\sigma(x^k, y^k; \lambda^k) - L_\sigma(x^{k+1}, y^k; \lambda^k) \geq \frac{\eta}{2} \|x^k - x^{k+1}\|^2. \quad (18)$$

Moreover, since y^{k+1} minimizes the y -subproblem (11c), we have

$$L_\sigma(x^{k+1}, y^k; \lambda^{k+\frac{1}{2}}) - L_\sigma(x^{k+1}, y^{k+1}; \lambda^{k+\frac{1}{2}}) \geq 0. \quad (19)$$

From the definition of the augmented Lagrangian function $L_\sigma(\cdot)$ in (10), we deduce

$$\begin{aligned} & L_\sigma(x^{k+1}, y^k; \lambda^k) - L_\sigma(x^{k+1}, y^k; \lambda^{k+\frac{1}{2}}) \\ & + L_\sigma(x^{k+1}, y^{k+1}; \lambda^{k+\frac{1}{2}}) - L_\sigma(x^{k+1}, y^{k+1}; \lambda^{k+1}) \\ & = (\lambda^k - \lambda^{k+\frac{1}{2}})^\top (y^k - Rx^{k+1}) + (\lambda^{k+\frac{1}{2}} - \lambda^{k+1})^\top (y^{k+1} - Rx^{k+1}) \\ & = (\lambda^k - \lambda^{k+1})^\top (y^{k+1} - Rx^{k+1}) + \theta \sigma (y^k - Rx^{k+1})^\top (y^{k+1} - y^k). \end{aligned} \quad (20)$$

Adding (11b) and (11d), we get

$$y^k - Rx^{k+1} = \frac{1}{(\theta+1)\sigma} (\lambda^{k+1} - \lambda^k) - \frac{1}{\theta+1} (y^{k+1} - y^k), \quad (21)$$

and

$$y^{k+1} - Rx^{k+1} = \frac{1}{(\theta+1)\sigma} (\lambda^{k+1} - \lambda^k) + \frac{\theta}{\theta+1} (y^{k+1} - y^k). \quad (22)$$

Substituting (21) and (22) into (20), we obtain

$$\begin{aligned}
& L_\sigma(x^{k+1}, y^k; \lambda^k) - L_\sigma(x^{k+1}, y^k; \lambda^{k+\frac{1}{2}}) \\
& + L_\sigma(x^{k+1}, y^{k+1}; \lambda^{k+\frac{1}{2}}) - L_\sigma(x^{k+1}, y^{k+1}; \lambda^{k+1}) \\
= & -\frac{1}{(\theta+1)\sigma} \|\lambda^{k+1} - \lambda^k\|^2 - \frac{\theta\sigma}{\theta+1} \|y^{k+1} - y^k\|^2.
\end{aligned} \tag{23}$$

Summing up (18), (19), and (23) gives rise to

$$\begin{aligned}
& L_\sigma(x^k, y^k; \lambda^k) - L_\sigma(x^{k+1}, y^{k+1}; \lambda^{k+1}) \\
\geq & \frac{\eta}{2} \|x^{k+1} - x^k\|^2 - \frac{1}{(\theta+1)\sigma} \|\lambda^{k+1} - \lambda^k\|^2 - \frac{\theta\sigma}{\theta+1} \|y^{k+1} - y^k\|^2.
\end{aligned} \tag{24}$$

Under the assumption that the sequence $\{\lambda^k\}$ is bounded and the set \mathcal{X} is bounded, it follows from (21) or (22) that the sequence $\{y^k\}$ is also bounded. Therefore, $L_\sigma(x^k, y^k; \lambda^k)$ is bounded. Summing up (24) on both sides for k from 0 to ∞ , we have

$$\frac{\eta}{2} \sum_{k=0}^{\infty} \|x^{k+1} - x^k\|^2 < \infty + \frac{1}{(\theta+1)\sigma} \sum_{k=0}^{\infty} \|\lambda^{k+1} - \lambda^k\|^2 + \frac{\theta\sigma}{\theta+1} \sum_{k=0}^{\infty} \|y^{k+1} - y^k\|^2.$$

Moreover, according to Assumption 4, we know $\frac{\theta\sigma}{\theta+1} \sum_{k=0}^{\infty} \|y^{k+1} - y^k\|^2 < \infty$, therefore, we get $\|y^{k+1} - y^k\| \rightarrow 0$ as $k \rightarrow \infty$. This, together with the assumption that $\sum_{k=0}^{\infty} \|\lambda^{k+1} - \lambda^k\|^2 < \infty$, implies $\sum_{k=0}^{\infty} \|x^{k+1} - x^k\|^2 < \infty$, which further yields $\|x^{k+1} - x^k\| \rightarrow 0$ as $k \rightarrow \infty$. Using $\sum_{k=0}^{\infty} \|\lambda^{k+1} - \lambda^k\|^2 < \infty$ again, we have $\lambda^{k+1} - \lambda^k \rightarrow 0$. Then, (21) and (22) further imply

$$y^k - Rx^{k+1} \rightarrow 0, \tag{25}$$

and

$$y^{k+1} - Rx^{k+1} \rightarrow 0. \tag{26}$$

Since the x -subproblem is globally solved, we must have

$$0 \in 2 \sum_{i=1}^N C_i x^{k+1} - \sigma R^\top \left(y^k - Rx^{k+1} + \frac{\lambda^k}{\sigma} \right) + M(x^{k+1} - x^k) + N_{\mathcal{X}}(x^{k+1}). \tag{27}$$

Note that (17) implies

$$0 \in R^\top \partial \Omega(y^{k+1}) + \sigma R^\top \left(y^k - Rx^{k+1} + \frac{\lambda^{k+\frac{1}{2}}}{\sigma} \right) + \sigma R^\top (y^{k+1} - y^k). \tag{28}$$

From (27) and (28), we deduce that

$$\begin{aligned} 0 \in & R^\top \partial \Omega(y^{k+1}) + 2 \sum_{i=1}^N C_i x^{k+1} + M(x^{k+1} - x^k) + N_{\mathcal{X}}(x^{k+1}) \\ & + \sigma R^\top (y^{k+1} - y^k) + \alpha \sigma R^\top (y^k - Rx^{k+1}). \end{aligned}$$

This, together with (25), Lemma 3 and the fact that the normal cone of a closed set is outer semicontinuous set-valued mapping [49, Proposition 6.6], yields

$$0 \in R^\top \partial \Omega(y^*) + 2 \sum_{i=1}^N C_i x^* + M(x^* - x^k) + N_{\mathcal{X}}(x^*),$$

where (x^*, y^*) is any accumulation point of $\{(x^k, y^k)\}$. Additionally, note that (25) implies $y^* = Rx^*$. The proof is completed. \square

5 Extension to ESG-based behavioral portfolio optimization

With the deepening of the concept of sustainable development, the rise of Environmental, Social, and Governance (ESG) investing has become a significant feature of global financial markets. ESG provides investors with a more profound and comprehensive perspective on corporate performance by conducting a comprehensive assessment of companies in terms of the environment, society, and governance. ESG factors focus on a company's ecological footprint, social responsibility, and internal structure and transparency, forming the cornerstone of ESG investing [50]. Against the backdrop of the evolving global financial markets, ESG investing is gradually becoming the focus of the investment community. More and more investors realize that incorporating ESG factors into the investment decision-making process not only aligns with ethical and social responsibility requirements but also helps reduce investment risks and enhance long-term returns [51, 52]. This paper takes this as a starting point and, using the A55 dataset as an example, incorporates ESG factors into the investment decision-making process through a linear weighting approach. Next, we will explain in detail how to integrate ESG factors into the measurement of returns and risks.

To incorporate ESG into returns, we linearly combine traditional asset returns and ESG scores into ESG value returns by introducing the ESG affinity parameter τ . Following the approach of Wu et al. [39], $\tau \in [0, 1]$ is the affinity parameter, and its value is determined by the investor's ESG preferences. We denote $ESG_{i,t}$ as the ESG score of asset i at time t and $\varsigma_{i,t}$ as the standardized ESG score of asset i at time t . Since the components of ESG value returns have different update frequencies (ESG scores are typically updated annually, while returns have a much higher frequency), we use the "forward-filling" method [53]: if there is no single-period data update, the previous period's data is used for calculation, filling low-frequency data into high-frequency data. Because the ESG scores used in this paper come from Wind, com-

posed of management practice scores (total score of 7) and controversy event scores (total score of 3), the ESG scores range from 0 to 10. Therefore, we standardize them using the following method:

$$\varsigma_{i,t} = \frac{ESG_{i,t}}{5} - 1.$$

The standardized ESG scores range from [-1,1]. Normalized ESG scores have a positive (negative) impact on assets with ESG scores above (below) some “average” value on the original scale. For any $\tau \in [0, 1]$, the ESG value return can be defined as follows:

$$\zeta_{i,t}(\tau) = \tau \frac{\varsigma_{i,t}}{c} + (1 - \tau)r_{i,t},$$

where $r_{i,t}$ represents the return of asset i at time t , a constant $c \in \mathbb{R}$ is introduced to ensure that $\varsigma_{i,t}$ and $r_{i,t}$ are comparable. The value of c depends on the time scenario of the return; since this paper considers daily returns, a value of $c = 242$ is used to approximate the number of trading days in a year. The larger the value of τ , the more the investor cares about the impact of ESG on the portfolio and the less they care about asset returns; when $\tau = 0$, the investor does not consider ESG factors at all.

After incorporating ESG factors, the portfolio problem (7) can be reformulated as follows:

$$\min_{\mathbf{x}} \quad \sum_{i=1}^N \mathbf{x}^\top \widetilde{C}_i \mathbf{x} - \sum_{i=1}^N \alpha_i U\left((\widetilde{R}\mathbf{x})_{[i]}\right) \quad \text{s.t. } \mathbf{x} \in \mathcal{X},$$

where \mathcal{X} is the feasible set for the decision variable \mathbf{x} , $\mathcal{X} = \{\mathbf{x} : x_i \geq 0, i = 1, 2, \dots, m + d^*, \sum_{i=1}^{m+d^*} x_i + \kappa d^* = \xi_{init}\}$. Here, $\widetilde{R} = [\zeta_1^\top, \zeta_2^\top, \dots, \zeta_n^\top]^\top$, $\widetilde{C}_j \in \mathbb{R}^{(m+d^*) \times (m+d^*)}$ represents the covariance matrix calculated from ESG valued returns. We can then use the algorithm as model (7) to solve the above problem; details are not elaborated in this section.

6 Numerical experiments

This section is dedicated to the validation of the effectiveness of model (7) and the SADMM using real stock datasets. All numerical experiments presented in this paper are executed on a 64-bit laptop running Windows 10, equipped with an Intel(R) Core(TM) i5-8250U CPU @ 1.60 GHz 1.80 GHz, 8GB RAM, and MATLAB 2021a as the operating environment.

In our experimental design, we meticulously select four datasets: A55, consisting of 55 stocks from the Chinese A-share market, encompassing daily returns spanning from July 2019 to December 2021; NDX100, representing the U.S. NASDAQ 100 Index, with exclusions made for stocks with missing data, resulting in a dataset

comprising 95 stocks with daily returns recorded from January 2020 to June 2022; FTES100, mirroring the UK FTSE 100 Index, similarly excluding stocks with missing data, and comprising 98 stocks with daily returns from January 2020 to June 2022; and SP500, representing the U.S. Standard & Poor's 500 Index. For the SP500 dataset, given the dynamic nature of constituent stocks over time [25], we opt for daily returns from April 2011 to August 2013, a scenario during which the constituent stocks remained consistent.

The PSO algorithm is implemented by Matlab, taking advantage of its computational efficiency for discrete optimization. The objective function $-\tilde{D}_e(d)$ is evaluated for each particle, incorporating the recursion of the statistical properties of the new assets defined in (4). The parameters used for the implementation of the PSO include a swarm size of $n = 10$, a maximum number of iterations $K_{\max} = 100$, an inertia weight $\varpi = 0.5$, a cognitive coefficient $\varsigma_1 = 1.5$, a social coefficient $\varsigma_2 = 1.5$ and a maximum velocity $\vartheta_{\max} = 5$.

Building upon the methodology established by Tversky and Kahneman [7], we designate the parameters in our model as $\mu = 2.25$, $\alpha = \varrho = 0.88$, $\gamma = 0.69$, $\delta = 0.61$, and $B = 0$. To enhance convergence, we employ a dynamic update strategy for the penalty parameter σ as follows:

$$\sigma^{k+1} = \begin{cases} \iota\sigma^k, & \text{if } \|y^{k+1} - Rx^{k+1}\| > \epsilon_1, \\ \sigma^k, & \text{otherwise,} \end{cases}$$

immediately following the update of λ , where $\iota > 1$ is a constant [25]. The iterative process halts when both the original condition $\|y^k - Rx^k\| < \epsilon_1$ and the dual condition $\|y^k - y^{k-1}\| < \epsilon_2$ are simultaneously satisfied. It is crucial to note that, when selecting the optimal parameter θ , to ensure convergence within the proper range, we appropriately relax the original feasibility condition and dual feasibility condition to $\epsilon_1 = \epsilon_2 = 5 \times 10^{-3}$. In subsequent experiments aimed at enhancing solution accuracy, we set $\epsilon_1 = \epsilon_2 = 5 \times 10^{-4}$. The initial values are specified as $\sigma_0 = 1$, $\iota = 3$, and $r_f = 1.03 \times 10^{-2}$. Additionally, the maximum number of allowed iterations is set to 1000.

6.1 Numerical performance of SADMM

The initial phase of our experimentation entails utilizing four datasets to assess the efficacy of the SADMM. This study employs SADMM to derive optimal solutions for constructing investment portfolios. Initially, we conduct tests to assess the impact of the parameter θ in SADMM on solving non-convex feasibility problems. Specifically, we explore θ within the set $\{-1, -0.9, -0.7, -0.5, -0.3, -0.1, 0, 0.1, 0.3, 0.5, 0.7, 0.9, 1\}$ to evaluate the performance of the SADMM algorithm.

Table 1 presents the number of iteration steps (Iter.) and CPU calculation time in seconds (Time) corresponding to different choices of θ . The results reveal that SADMM demonstrates swift convergence in certain scenarios but fails to converge in others, validating the theoretical convergence range of the algorithm. Notably, when

Table 1 Numerical results of SADMM with different values of θ

θ	A55		NDX100		FTSE100		SP500	
	Iter	Time	Iter	Time	Iter	Time	Iter	Time
-1	1000	16.0280	822	61.2740	1000	203.2050	1000	66.7730
-0.9	1000	14.536000	42	3.4690	52	47.3630	1000	78.7450
-0.7	42	1.7200	42	3.4600	42	30.9670	1000	71.0260
-0.5	34	1.3740	42	4.1580	106	86.4990	1000	47.5950
-0.3	49	1.6750	42	3.5040	35	50.5370	1000	39.9780
-0.1	32	1.3420	52	4.1070	32	56.1490	63	5.3150
0	32	1.3460	62	4.8610	32	48.1760	62	5.1710
0.1	32	1.3890	32	2.7950	32	34.4350	62	5.1630
0.3	32	1.3100	32	2.8320	32	37.9140	182	22.9920
0.5	54	1.9230	32	2.8700	44	47.2600	53	4.8420
0.7	22	1.2120	32	2.9360	22	28.4580	52	4.7920
0.9	31	1.6790	32	2.8680	31	31.7090	58	6.4370
1	42	1.9080	42	3.6730	42	39.7440	1000	60.5690

Table 2 Numerical results for dataset of A55 under exploration or non-exploration

N	m	d^*	With exploration			Without exploration		
			Total	Obj. (10^{-2})	SR	Std (10^{-2})	Obj. (10^{-2})	SR
100	55	2	57	0.5114	1.5295	0.7705	0.7242	0.8527
200	55	1	56	1.2088	1.4432	1.2849	1.4131	0.0995
300	55	2	57	1.0072	2.9350	1.2074	1.4093	1.4982
400	55	2	57	0.9943	3.1313	1.1655	1.4147	1.3018
500	55	2	57	0.9151	3.8499	1.1201	1.3221	1.6881
600	55	2	57	0.8695	4.2799	1.0723	1.2389	1.8459

θ is set to 0.7, the algorithm exhibits the fewest iterations and requires the least CPU computing time.

A comprehensive evaluation involves comparing our method with alternative approaches. We juxtapose our method with the classic alternating direction method of multipliers (ADMM) adopted by Corsaro et al. [54] ($\theta = 0$) and the strictly contracted Peaceman-Rachford splitting method proposed by He et al. [32] ($\theta = 1$). Furthermore, Table 1 illustrates trends in the number of iteration steps and CPU computing time for different θ values. It is noteworthy that the case $\theta > 0$ outperforms the others. Based on the test results, we choose $\theta = 0.7$ for subsequent experiments.

6.2 Numerical performance of the model

In this subsection, we test the performance of the model with or with exploration on several datasets. Specifically, Tables 2, 3, 4, 5 present the numerical results of exploration and non-exploration scenarios for each of the four datasets. In these tables, “ d^* ” denotes the count of new assets acquired through exploration, while “Total” represents the overall number of assets in the expanded investment portfolio. This total encompasses both known assets (m) and newly acquired assets (d^*). A careful examination of these tables reveals variations in the number of newly explored assets

Table 3 Numerical results for dataset of NDX100 under exploration or non-exploration

N	m	d^*	With exploration			Without exploration			
			Total	Obj. (10^{-2})	SR	Std (10^{-2})	Obj. (10^{-2})	SR	Std (10^{-2})
100	95	1	96	2.0568	0.9833	2.2527	2.3442	0.7339	2.4424
200	95	3	98	1.1593	2.8977	1.5776	1.8339	1.3399	2.0004
300	95	3	98	1.0069	3.4028	1.3973	1.7272	1.3278	1.8433
400	95	3	98	0.8487	4.3362	1.2369	1.4747	1.7978	1.5916
500	95	3	98	1.0254	3.2902	1.2474	1.5323	1.1248	1.5345
600	95	3	98	1.0329	3.3767	1.2410	1.6387	0.5367	1.5709

Table 4 Numerical results for dataset of FTSE100 under exploration or non-exploration

N	m	d^*	With exploration			Without exploration			
			Total	Obj. (10^{-2})	SR	Std (10^{-2})	Obj. (10^{-2})	SR	Std (10^{-2})
100	98	4	102	1.1233	1.3660	1.5849	2.4118	-0.2539	2.3548
200	98	1	99	1.5992	0.5589	1.7420	1.9111	-0.0427	1.9151
300	98	1	99	1.5990	0.4713	1.6884	1.7970	0.0295	1.8047
400	98	1	99	1.3714	0.9529	1.4963	1.5511	0.3771	1.5977
500	98	1	99	1.2630	1.2188	1.3727	1.4412	0.4901	1.4681
600	98	1	99	1.2759	0.7138	1.3072	1.4637	-0.0254	1.4001

Table 5 Numerical results for dataset of SP500 under exploration or non-exploration

N	m	d^*	With exploration			Without exploration			
			Total	Obj. (10^{-2})	SR	Std (10^{-2})	Obj. (10^{-2})	SR	Std (10^{-2})
100	458	1	459	0.9682	1.1169	1.3428	1.1768	0.5581	1.4515
200	458	2	460	0.5321	3.3899	1.0579	1.0895	1.1618	1.3163
300	458	2	460	0.3967	4.8792	0.9049	0.9155	1.6937	1.1236
400	458	2	460	0.3202	5.9408	0.8269	0.8810	1.6568	1.0441
500	458	2	460	0.2486	7.3618	0.7636	0.8902	1.9673	1.0561
600	458	1	449	0.7059	3.1986	0.9423	0.8876	2.1833	1.0215

resulting from diverse datasets. Over an investment scenarios of 100, A55 yields 2 new assets, while NDX100 and SP500 each contribute 1 new asset, and FTSE100 contributes 1 new asset as well. Moreover, even within the same dataset and under different investment scenarios, variations exist in the count of newly acquired assets. For instance, in A55, except for an investment scenarios of 200, which results in 1 new asset, all other scenarios yield 2 new assets. Nonetheless, the differences in the count of new assets under distinct investment scenarios for the same dataset are generally modest and exhibit relative stability. This observation underscores the connection between the number of new assets acquired through exploration and the return rate of existing assets or datasets. Building upon known assets, diverse datasets can realize additional gains by incurring exploration costs to uncover new assets during various investment scenarios. This strategic exploration can identify new investment opportunities, thereby enhancing investment efficiency and mitigating risks, ultimately leading to the formulation of an improved investment portfolio.

Subsequently, we compute optimal investment portfolios for scenarios involving the exploration and non-exploration of new assets across the four datasets and dif-

ferent investment scenarios. Performance indicators such as the optimal objective function value (Obj.), Sharpe ratio (SR), and standard deviation (Std) are employed for summarizing their performance. Analysis of the tables reveals that the minimized objective function values obtained through the exploration of new assets in all four datasets are consistently smaller than those achieved solely by investing in known assets. Furthermore, considering the Sharpe ratio, the exploration of new assets consistently results in a higher Sharpe ratio compared to investing only in known assets, sometimes nearly doubling the latter. Lastly, from the perspective of standard deviation, portfolios constructed by exploring new assets exhibit smaller standard deviations compared to portfolios comprising only known assets. In conclusion, exploration of new assets leads to portfolios with superior objective function values, higher Sharpe ratios, and lower volatility.

Furthermore, we assess the performance of optimal portfolios across four datasets based on their cumulative returns over a 600-scenario investment horizon. In Fig. 3, the distinct solid lines depict the cumulative return of the optimal portfolio, considering new asset exploration, alongside the cumulative return of the optimal portfolio excluding new asset exploration. Observation of the figure reveals a consistent trend where, for a given dataset, the cumulative return curve associated with exploring new assets consistently outperforms that of not exploring new assets. As the investment scenario progresses, the cumulative return derived from exploring new assets consistently exceeds that from not exploring new assets, and the gap between the cumulative

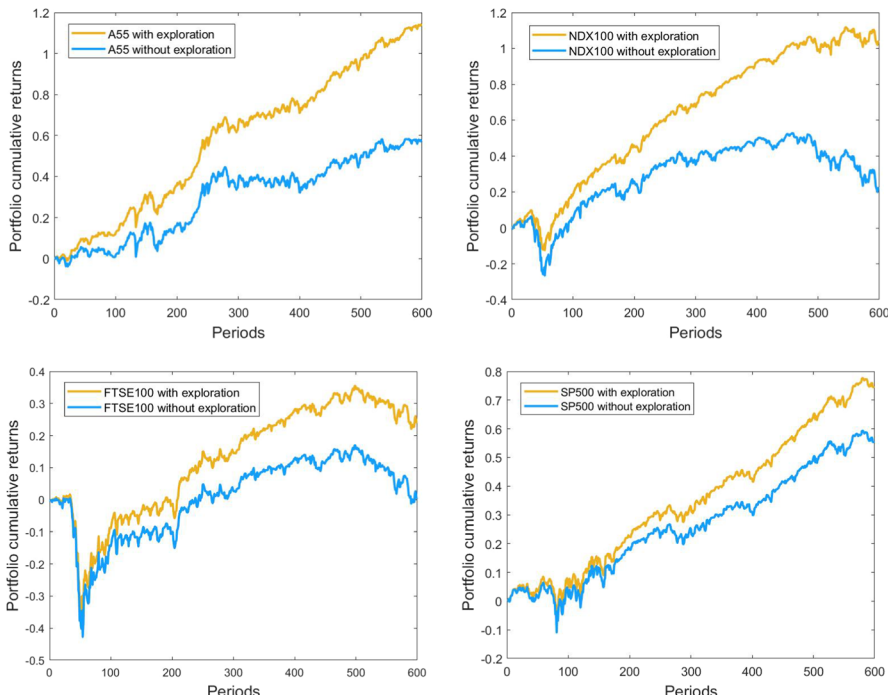


Fig. 3 The cumulative returns of different datasets during 600 scenarios under exploration or non-exploration

returns widens. This observation indicates a positive relationship between cumulative returns and the investment scenario; generally, longer investment scenarios tend to yield higher cumulative returns.

6.3 Numerical effect of ESG factor

In this subsection, we present the experimental results, taking into account ESG factors. In Table 6, we give the numerical outcomes of dataset A55, considering the influence of ESG, in both exploratory and non-exploratory scenarios. Table 6 reveals that, irrespective of the continued exploration of new assets, an escalating τ (indicative of increasing investor preference for ESG) corresponds to a declining trend in the objective function value and standard deviation of the optimal investment portfolio. Simultaneously, the Sharpe ratio displays an ascending trend.

Additionally, in Fig. 4, we depict the cumulative returns of the optimal investment portfolios for exploration and non-exploration scenarios of the A55 dataset under different scenarios investment horizon, accounting for the impact of ESG. The results illustrate that, at almost $\tau = 0.5$, the cumulative returns of the optimal investment portfolios for both exploring and nonexploring new assets reach their zenith. In summary, these observations underscore that a stronger inclination towards ESG cor-

Table 6 Numerical results for dataset of A55 under exploration or non-exploration

τ	N	m	d^*	With exploration			Without exploration			
				Total	Obj. (10^{-2})	SR	Std (10^{-2})	Obj. (10^{-2})	SR	Std (10^{-2})
0	100	55	2	57	0.5114	1.5295	0.7705	0.7242	0.8527	0.8650
	200	55	1	56	1.2088	1.4432	1.2849	1.4131	0.0995	1.3835
	300	55	2	57	1.0072	2.9350	1.2074	1.4093	1.4982	1.4073
	400	55	2	57	0.9943	3.1313	1.1655	1.4147	1.3018	1.3669
	500	55	2	57	0.9151	3.8499	1.1201	1.3221	1.6881	1.3125
	600	55	2	57	0.8695	4.2799	1.0723	1.2389	1.8459	1.2307
0.25	100	55	6	61	-0.1120	7.0266	0.4302	0.6253	0.2946	0.6736
	200	55	1	56	0.8948	1.8994	0.9742	1.0661	1.0843	1.0445
	300	55	1	56	0.8812	2.6236	0.9898	1.0555	1.7490	1.0634
	400	55	1	56	0.8760	2.7601	0.9606	1.0570	1.7139	1.0339
	500	55	1	56	0.8032	3.4723	0.9203	0.9800	2.1898	0.9911
	600	55	1	56	0.7628	3.9014	0.8823	0.9386	2.4619	0.9505
0.5	100	55	1	56	0.2341	1.9086	0.4189	0.3724	0.3915	0.4499
	200	55	3	58	0.3030	4.6163	0.5718	0.6876	1.4928	0.7006
	300	55	3	58	0.2872	5.8937	0.5794	0.6765	2.3288	0.7131
	400	55	3	58	0.2727	6.9642	0.5619	0.6748	2.4154	0.6945
	500	55	3	58	0.2230	8.4767	0.5377	0.6161	3.2376	0.6650
	600	55	3	58	0.1933	9.7679	0.5152	0.5827	3.7169	0.6376
0.75	100	55	2	57	-0.1770	7.8610	0.1927	0.0808	3.9891	0.2245
	200	55	3	58	-0.0298	7.9851	0.2889	0.2678	4.3361	0.3516
	300	55	3	58	-0.0369	11.4878	0.2937	0.2622	5.4216	0.3580
	400	55	3	58	-0.0502	13.7640	0.2857	0.2560	4.8230	0.3490
	500	55	1	56	0.1024	9.5584	0.3126	0.2179	5.7947	0.3340
	600	55	1	56	0.0808	10.7333	0.2997	0.1951	7.1059	0.3204

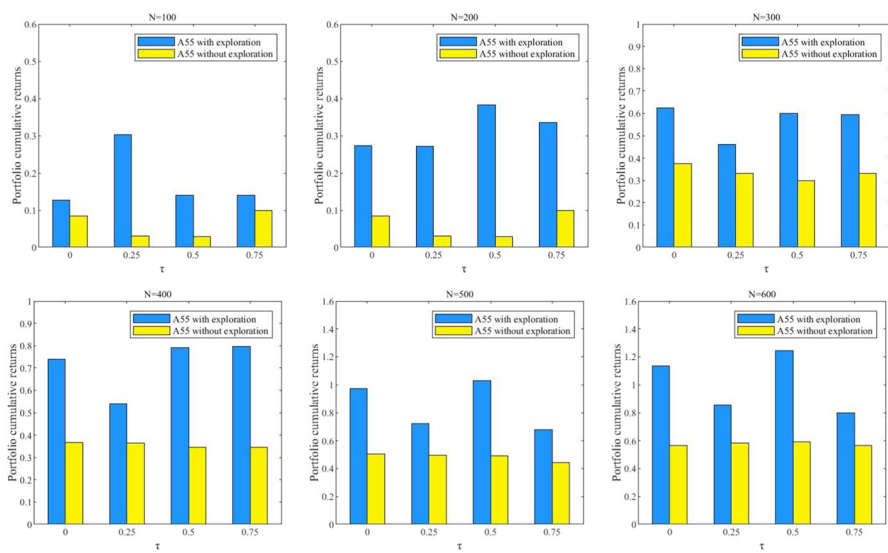


Fig. 4 The cumulative returns of A55 dataset during different scenarios under exploration or non-exploration considering ESG

relates with an increased Sharpe ratio in the optimal investment portfolio, decreased risk, and a positive influence of ESG on the investment portfolio. Similarly, when τ remains constant, a comparative analysis of the three metrics between exploring and not exploring new assets yields the same conclusions as the aforementioned experiment. The objective function value and standard deviation of the optimal investment portfolio in the exploratory scenario are markedly lower than those in the non-exploratory scenario, while the Sharpe ratio is notably higher. This underscores the imperative of seeking new investment opportunities within the existing scope to effectively enhance returns and mitigate risks.

7 Conclusions

Recognizing that investors' diverse attitudes toward gains and losses significantly influence investment decisions, we aim to depict investors' genuine attitudes and preferences accurately. To achieve this, we integrate the utility function of cumulative prospect theory with the mean-variance framework, crafting a behavioral portfolio model. This amalgamation of cumulative prospect theory into the traditional portfolio selection problem furnishes a more flexible tool for portfolio management. Moreover, in acknowledgment of the current uncertainties in investment landscapes, we discard the implicit assumption of a fixed number of available investment assets. We posit that investors possess the capability to broaden their investment universe by exploring novel assets. Our objective is to formulate a behavioral portfolio selection model endowed with an expandable investment horizon. Within the established mean-variance model framework, we introduce the utility function of cumulative prospect theory. This expansion accommodates not only traditional mean-variance

preferences but also addresses asymmetric risk preferences, considering investors' distinct attitudes toward gains and losses. Through this framework, we strike a harmonious balance between leveraging existing investment opportunities and exploring new ones to formulate an optimal investment strategy.

From a numerical standpoint, we employ the symmetric alternating direction method of multipliers and the pooling-adjacent-violators algorithm to solve the behavioral portfolio model, empirically showcasing the effectiveness and superiority of this solution methodology. On the experimental front, we conduct several experiments employing various real stock datasets to elucidate the advantages of behavioral portfolio models. Furthermore, considering the escalating concept of sustainable development, we extend the model by incorporating a linear combination of ESG ratings and traditional returns to generate ESG value returns. This extension explores ESG factors' influence on behavioral investment portfolios. Our findings indicate that diverse datasets can achieve additional benefits within the behavioral portfolio framework outlined in this article by incurring exploration costs during different investment scenarios to unearth new assets. This strategic exploration reveals new investment opportunities, thereby enhancing investment efficiency and mitigating risk, ultimately resulting in an improved investment portfolio. Additionally, ESG ratings effectively reduce portfolio risks, improve Sharpe ratios, deliver superior outcomes, and offer valuable insights into behavioral portfolio selection within the context of sustainable development. Subsequent research will be dedicated to examining the impacts of behavioral portfolio investments within the context of multi-scenario decision-making. Moreover, the integration of additional risk measures into the portfolio optimization process will be explored.

Acknowledgements We would like to express our gratitude to the associate editor and two anonymous referees for their helpful comments and the authors in [25] who generously shared their codes. Zhongming Wu acknowledges the National Natural Science Foundation of China (Nos. 12471291, 12001286), the Natural Science Foundation of Jiangsu Province (Grant No. BK20241899) and the Project funded by China Postdoctoral Science Foundation (No. 2022M711672). Valentina De Simone acknowledges the National Group for Scientific Computation (INdAM-GNCS) and the MIUR-PRIN 2022 Project "Numerical Optimization with Adaptive Accuracy and Applications to Machine Learning", project code: 2022N3ZNAX (CUP E53D2300 7700006), under the National Recovery and Resilience Plan (PNRR), Italy.

Funding Open access funding provided by Università degli Studi della Campania Luigi Vanvitelli within the CRUI-CARE Agreement.

Declarations

Conflict of interest The authors declare that they have no known competing financial interests or personal relationships that could have appeared to influence the work reported in this paper.

Open Access This article is licensed under a Creative Commons Attribution 4.0 International License, which permits use, sharing, adaptation, distribution and reproduction in any medium or format, as long as you give appropriate credit to the original author(s) and the source, provide a link to the Creative Commons licence, and indicate if changes were made. The images or other third party material in this article are included in the article's Creative Commons licence, unless indicated otherwise in a credit line to the material. If material is not included in the article's Creative Commons licence and your intended use is not permitted by statutory regulation or exceeds the permitted use, you will need to obtain permission directly from the copyright holder. To view a copy of this licence, visit <http://creativecommons.org/licenses/by/4.0/>

References

1. Bailey, W., Kumar, A., Ng, D.: Behavioral biases of mutual fund investors. *J. Financ. Econ.* **102**(1), 1–27 (2011)
2. Harris, R.D., Mazibas, M.: Portfolio optimization with behavioural preferences and investor memory. *Eur. J. Oper. Res.* **296**(1), 368–387 (2022)
3. Curtis, G.: Modern portfolio theory and behavioral finance. *J. Wealth Manag.* **7**(2), 16–22 (2004)
4. Bilbao-Terol, A., Arenas-Parra, M., Cañal-Fernández, V., Bilbao-Terol, C.: Multi-criteria decision making for choosing socially responsible investment within a behavioral portfolio theory framework: a new way of investing into a crisis environment. *Ann. Oper. Res.* **247**, 549–580 (2016)
5. Aquino, L.D.G., Sornette, D., Strub, M.S.: Portfolio selection with exploration of new investment assets. *Eur. J. Oper. Res.* **310**(2), 773–792 (2023)
6. Kai-Ineman, D., Tversky, A.: Prospect theory: an analysis of decision under risk. *Econometrica* **47**(2), 363–391 (1979)
7. Tversky, A., Kahneman, D.: Advances in prospect theory: cumulative representation of uncertainty. *J. Risk Uncertain.* **5**, 297–323 (1992)
8. He, X.D., Zhou, X.Y.: Portfolio choice under cumulative prospect theory: an analytical treatment. *Manage. Sci.* **57**(2), 315–331 (2011)
9. Fu, Y., Li, M.: Dea cross-efficiency aggregation based on preference structure and acceptability analysis. *Int. Trans. Oper. Res.* **29**(2), 987–1011 (2022)
10. Shi, Y., Cui, X., Yao, J., Li, D.: Dynamic trading with reference point adaptation and loss aversion. *Oper. Res.* **63**(4), 789–806 (2015)
11. Shefrin, H., Statman, M.: Behavioral portfolio theory. *J. Financ. Quantitat. Anal.* **35**(2), 127–151 (2000)
12. Luxenberg, E., Schiele, P., Boyd, S.: Portfolio optimization with cumulative prospect theory utility via convex optimization. *Comput. Econom.*, 1–21 (2024)
13. Shi, Y., Cui, X., Li, D.: Discrete-time behavioral portfolio selection under cumulative prospect theory. *J. Econ. Dyn. Control* **61**, 283–302 (2015)
14. Hens, T., Mayer, J.: Cumulative prospect theory and mean variance analysis: a rigorous comparison. Swiss Finance Institute Research Paper, 14–23 (2014)
15. Fulga, C.: Portfolio optimization under loss aversion. *Eur. J. Oper. Res.* **251**(1), 310–322 (2016)
16. Bi, J., Jin, H., Meng, Q.: Behavioral mean-variance portfolio selection. *Eur. J. Oper. Res.* **271**(2), 644–663 (2018)
17. Best, M.J., Hlouskova, J.: The efficient frontier for bounded assets. *Math. Methods Oper. Res.* **52**, 195–212 (2000)
18. Zakamulin, V.: Sharpe (ratio) thinking about the investment opportunity set and capm relationship. *Econom. Res. Int.* **2011**(1), 781760 (2011)
19. Daw, N.D., Odoherty, J.P., Dayan, P., Seymour, B., Dolan, R.J.: Cortical substrates for exploratory decisions in humans. *Nature* **441**(7095), 876–879 (2006)
20. Wang, L., Chen, K., Chiu, M.C., Wong, H.Y.: Optimal expansion of business opportunity. *Eur. J. Oper. Res.* **309**(1), 432–445 (2023)
21. Markowitz, H.M., Todd, G.P.: Mean-Variance Analysis in Portfolio Choice and Capital Markets. Wiley, Hoboken (2000)
22. Steinbach, M.C.: Markowitz revisited: mean-variance models in financial portfolio analysis. *SIAM Rev.* **43**(1), 31–85 (2001)
23. Corsaro, S., De Simone, V.: Adaptive ℓ_1 -regularization for short-selling control in portfolio selection. *Comput. Optim. Appl.* **72**(2), 457–478 (2019)
24. Mousavi, A., Michailidis, G.: Cardinality constrained mean-variance portfolios: A penalty decomposition algorithm. *Comput. Optim. Appl.*, 1–18 (2025)
25. Cui, X., Jiang, R., Shi, Y., Xiao, R., Yan, Y.: Decision making under cumulative prospect theory: An alternating direction method of multipliers. *INFORMS J. Comput.*, 1–18 (2024)
26. Bai, J., Zhang, M., Zhang, H.: An inexact admm for separable nonconvex and nonsmooth optimization. *Comput. Optim. Appl.* **90**, 445–479 (2025)

27. Wu, Z., Li, M., Wang, D.Z., Han, D.: A symmetric alternating direction method of multipliers for separable nonconvex minimization problems. *Asia-Pacific J. Oper. Res.* **34**(06), 1750030 (2017)
28. Boyd, S., Parikh, N., Chu, E., Peleato, B., Eckstein, J.: Distributed optimization and statistical learning via the alternating direction method of multipliers. *Foundations Trends® Mach Learn* **3**(1), 1–122 (2011)
29. Cai, X., Guo, K., Jiang, F., Wang, K., Wu, Z., Han, D.: The developments of proximal point algorithms. *J. Operat. Res. Soc. China* **10**(2), 197–239 (2022)
30. Han, D.: A survey on some recent developments of alternating direction method of multipliers. *J. Operat. Res. Soc. China* **10**(1), 1–52 (2022)
31. Gabay, D., Mercier, B.: A dual algorithm for the solution of nonlinear variational problems via finite element approximation. *Comput. Math. Appl.* **2**(1), 17–40 (1976)
32. He, B., Liu, H., Wang, Z., Yuan, X.: A strictly contractive peaceman-rachford splitting method for convex programming. *SIAM J. Optim.* **24**(3), 1011–1040 (2014)
33. He, B., Ma, F., Yuan, X.: Convergence study on the symmetric version of admm with larger step sizes. *SIAM J. Imag. Sci.* **9**(3), 1467–1501 (2016)
34. Jing, K., Xu, F., Li, X.: A bi-level programming framework for identifying optimal parameters in portfolio selection. *Int. Trans. Oper. Res.* **29**(1), 87–112 (2022)
35. Bai, J., Li, J., Xu, F., Zhang, H.: Generalized symmetric admm for separable convex optimization. *Comput. Optim. Appl.* **70**(1), 129–170 (2018)
36. Bai, J., Chen, Y., Yu, X., Zhang, H.: Generalized asymmetric forward-backward-adjoint algorithms for convex-concave saddle-point problem. *J. Sci. Comput.* **102**(3), 80 (2025)
37. Guo, K., Han, D., Wu, T.: Convergence of alternating direction method for minimizing sum of two nonconvex functions with linear constraints. *Int. J. Comput. Math.* **94**(8), 1653–1669 (2017)
38. Xu, F., Li, X., Dai, Y.-H., Wang, M.: New insights and augmented lagrangian algorithm for optimal portfolio liquidation with market impact. *Int. Trans. Oper. Res.* **30**(5), 2640–2664 (2023)
39. Wu, Z., Yang, L., Fei, Y., Wang, X.: Regularization methods for sparse ESG-valued multi-period portfolio optimization with return prediction using machine learning. *Expert Syst. Appl.* **232**, 120850 (2023)
40. Bai, X., Sun, J., Zheng, X.: An augmented lagrangian decomposition method for chance-constrained optimization problems. *INFORMS J. Comput.* **33**(3), 1056–1069 (2021)
41. Ayer, M., Brunk, H.D., Ewing, G.M., Reid, W.T., Silverman, E.: An empirical distribution function for sampling with incomplete information. *Ann. Math. Stat.*, 641–647 (1955)
42. Brunk, H.D., Barlow, R.E., Bartholomew, D.J., Bremner, J.M.: Statistical inference under order restrictions: the theory and application of isotonic regression. *Int. Stat. Rev.* **41**, 395 (1973)
43. Ahuja, R.K., Orlin, J.B.: A fast scaling algorithm for minimizing separable convex functions subject to chain constraints. *Oper. Res.* **49**(5), 784–789 (2001)
44. Cui, Z., Lee, C., Zhu, L., Zhu, Y.: Non-convex isotonic regression via the myersonian approach. *Stat. Prob. Lett.* **179**, 109210 (2021)
45. Clarke, F.H.: Optim. Nonsmooth Anal. SIAM, Philadelphia (1990)
46. Beck, A.: First-Order Methods in Optimization. SIAM, Philadelphia (2017)
47. Wang, Y., Yin, W., Zeng, J.: Global convergence of admm in nonconvex nonsmooth optimization. *J. Sci. Comput.* **78**, 29–63 (2019)
48. Xu, Y., Yin, W., Wen, Z., Zhang, Y.: An alternating direction algorithm for matrix completion with nonnegative factors. *Front. Math. China* **7**, 365–384 (2012)
49. Rockafellar, R.T., Wets, R.J.-B.: Variational Analysis, vol. 317. Springer, New York (2009)
50. Widyawati, L.: A systematic literature review of socially responsible investment and environmental social governance metrics. *Bus. Strateg. Environ.* **29**(2), 619–637 (2020)
51. Utz, S., Wimmer, M., Steuer, R.E.: Tri-criterion modeling for constructing more-sustainable mutual funds. *Eur. J. Oper. Res.* **246**(1), 331–338 (2015)
52. Pedersen, L.H., Fitzgibbons, S., Pomorski, L.: Responsible investing: the ESG-efficient frontier. *J. Financ. Econ.* **142**(2), 572–597 (2021)
53. Lauria, D., Lindquist, W.B., Mittnik, S., Rachev, S.T.: ESG-valued portfolio optimization and dynamic asset pricing. Preprint at [arXiv:2206.02854](https://arxiv.org/abs/2206.02854) (2022)
54. Corsaro, S., De Simone, V., Marino, Z.: Fused LASSO approach in portfolio selection. *Ann. Oper. Res.* **299**(1), 47–59 (2021)

Authors and Affiliations

Zhongming Wu¹ · Liu Yang¹ · Valentina De Simone² 

✉ Valentina De Simone
valentina.desimone@unicampania.it

Zhongming Wu
wuzm@nuist.edu.cn

Liu Yang
202212420007@nuist.edu.cn

¹ School of Management Science and Engineering, Nanjing University of Information Science and Technology, Nanjing 210044, China

² Department of Mathematics and Physics, University of Campania “Luigi Vanvitelli”, 81100 Caserta, Italy